Self-organization of topological defects due to applied constraints

Jonathan H. McCoy,[1,*] Will Brunner,[2] Werner Pesch,[3] and Eberhard Bodenschatz[4,1,†]

[1] *Department of Physics, Cornell University, Ithaca, NY 14853, USA*
[2] *inXitu, inc., Mountain View, CA 94043, USA*
[3] *Department of Physics, University of Bayreuth, Bayreuth, Germany*
[4] *Max Planck Institute for Dynamics and Self-Organization, Göttingen, Germany*

(Dated: November 10, 2008)

While topological defects are essential to our understanding of self-organizing periodic systems, little is known about how these systems respond when their defects are subjected to geometrical constraints. In an experiment on spatially modulated thermal convection patterns, we observe that applied geometrical constraints bind topological defects into robust self-localized structures that evolve through aggregation, annihilation, and self-replication. We demonstrate that this unexpected cooperative response to the modulation is a natural consequence of three generic elements: phase-locking, symmetry-breaking, and spatial resonance.

PACS numbers: 05.45.Jn, 47.54.-r, 47.55.P-, 89.75.Fb

The self-organization of ordered structures is a recurring theme in physics, chemistry, and biology [1–3]. Spatially periodic patterns, in particular, are observed at length scales ranging from the atomic to the astronomical. Self-organized patterns are rarely perfect; topological defects, such as dislocations and disclinations, are an intrinsic element of their phenomenology [3, 4]. Topological defects have a spatially localized core region where the background pattern is torn, surrounded by a far field region where the pattern is only weakly distorted; like electric charge, these topologically charged distortions can be detected by measurements made on any loop (or surface) enclosing their core [3, 4]. These properties make topological defects essential to our understanding of pattern selection, creep and yield phenomena, order-disorder transitions, and the mechanisms underlying spatiotemporal chaos [3–8]. This raises the interesting question of how self-organizing systems respond when topological defects are subjected to geometrical constraints, restricting their formation and dynamics.

The formal connection between topological defects and spontaneously broken symmetries [3, 4] suggests that an externally broken symmetry, *e.g.* a spatial modulation, may be used to constrain defects. We find, in an experiment on spatially modulated thermal convection, that constrained defects create a significant departure from the standard pattern selection paradigm [3]. Weakly convecting patterns are completely phase-locked to the modulation. This frustrates the system if the imposed pattern would be unstable in the absence of modulation. Defect nucleation generally provides the system with a means of adjusting its wave vector field. Here, however, this selection mechanism is partially blocked and thus controlled by the modulation. Instead of merely breaking up and/or adjusting a spatially periodic state, defects enable the modulated system to self-organize new types of periodic structures. These structures, shown in Fig. 1, are crystalline lattices embedded in a periodic background pattern. Some of the lattices are ladder-like, extended in one direction and strongly confined in another. Yet, as shown later, all are constructed from a common reciprocal basis set. The formation of such structures cannot be described using known theoretical frameworks [9].

Our experiments illustrate how constrained defects can cooperate in completely unexpected ways. Dislocations in the pattern are pinned and their far-field distortions are confined to spatially localized domains with zero net charge, converting a geometrical constraint into a topological one. The smallest possible structure produced by this mechanism is a new type of charge neutral defect, a localized orientational defect, which is never observed in the absence of modulation. We interpret the localized domains of Fig. 1 as crystalline aggregates of these orientational defects. As many papers have emphasized in recent years, localized structures that are *not* topological in nature can spontaneously appear and disappear [10–13], self-replicate [12–14], and even aggregate to form molecular clusters and crystals [14–17]. Our experiment offers the first opportunity to observe these striking self-organization behaviors in a setting where topological defects are the essential dynamical agents. In this Letter, we demonstrate that localization, crystalline order, and pattern-forming dynamical motifs (aggregation, annihilation, and self-replication) are natural consequences of three generic elements: phase-locking, symmetry-breaking, and spatial resonance.

When a thin, horizontal fluid layer is driven out of equilibrium by heating from below and cooling from above, circulating spatially periodic flow patterns self-organize; this buoyancy-driven flow, known as Rayleigh-Bénard convection, is one of the archetypical examples of pattern formation in nature [6]. The physics can be captured by three non-dimensional parameters: the Rayleigh number Ra, which is proportional to the applied temperature difference, compares the effects of buoyancy and dissipation, the Prandtl number Pr compares viscous and ther-

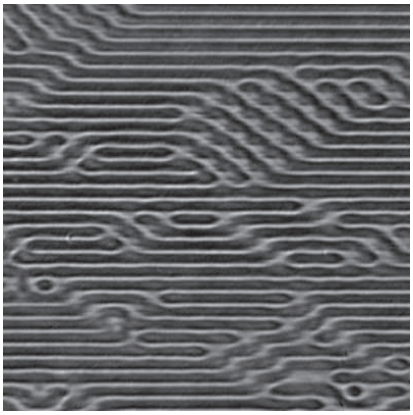

FIG. 1: A shadowgraph image of localized structures in a spatially modulated thermal convection pattern ($Ra \sim 1.9$ Ra_c). Movies showing the spatiotemporal evolution of these structures are available at Ref. [21].

mal diffusion, and the third parameter is the magnitude of the pattern's local wave vector $\mathbf{k} = (k_x, k_y)$. Below a universal critical value Ra_c, there is no fluid motion. For Ra above Ra_c and fixed Pr, convection patterns are stable for $\mathbf{k}$ lying within a well-characterized annulus in the wave vector plane [3]. This annulus defines the preferred periodicities of the system, even when the pattern is spatiotemporally chaotic [6]. In our experiment, we frustrate this system by imposing a spatially periodic modulation with a wave vector $\mathbf{K}_0$ lying close to but *outside* of the stability annulus.

Our experiment was performed on a thin layer of compressed SF_6 gas, in an apparatus essentially identical to that described in [18]. This layer was bounded above by an optically-flat, single-crystal sapphire window, providing optical access for pattern visualization, and bounded below by an optically-flat silicon mirror. The temperatures of the silicon and sapphire plates were regulated independently to $\pm$ 0.0004 °C. The pressure was held constant at (1.722 $\pm$ 0.030) MPa, regulated to $\pm$ 0.3 kPa, and the mean temperature in the layer was held at (21.00 $\pm$ 0.02) °C. Under these circumstances, SF_6 has Prandtl number $Pr \sim 0.9$. We introduced a permanent spatial modulation by microfabricating a periodic array of parallel SU-8 polymer ridges on the bottom plate. These ridges drive observable upflow of fluid, forcing the pattern to phase-lock to the imposed periodicity [19]. The ridges were 65 μm high and 100 μm wide, with one ridge per mm. The thickness of the layer, for comparison, was $d = (596 \pm 27)$ μm. The characteristic thermal diffusion time for this layer, $\tau_v = d^2/\kappa$, where κ is the thermal diffusivity of the gas, is 2.5 sec. Flow patterns were confined by an annular boundary of diameter $L = 110d$. The aspect ratio, $\Gamma = L/(2d)$, provides a characteristic time, $\tau_h = \Gamma^2\tau_v = 3025\tau_v$, associated with system-scale pattern relaxations [6]. Alternation between warmer regions where gas is rising and cooler regions where it is sinking sets up a spatially varying index of refraction, which we visualize by passing collimated monochromatic light through the fluid and imaging the near-field diffraction pattern. This "shadowgraph" technique is described in detail elsewhere [18, 20].

Our spatial modulation scheme breaks the rotational isotropy and one of the two space translational symmetries of the fluid layer. As a result, a convection pattern is present even for $Ra < Ra_c$. Below $\sim$1.6 Ra_c, the entire pattern is spatially phase-locked to the imposed modulation. Near $\sim$1.6 Ra_c, localized domains of obliquely-oriented stripes begin to nucleate at the boundaries. These domains do not grow to fill the bulk of the pattern. Instead, narrow sections of stripes peel off from the boundaries and invade the bulk. Over time, a perpetually reorganizing but *steady-state* population of localized structures builds up in the bulk [19]. The spatiotemporal evolution of these structures is rapid compared to the system-scale relaxation time τ_h, but slow compared to the thermal diffusion time τ_v [21]. This separation of scales demonstrates that the boundaries have only a weak influence on the bulk dynamics. We focus here on the steady-state behavior observed away from the boundaries at $Ra \sim 1.9$ Ra_c. A typical pattern observed in this regime is shown in Fig. 1. The localized structures in these patterns have crystalline order but the dynamics are spatiotemporally chaotic. To highlight this unusual twist on the classic theme of order within chaos, we describe this state as exhibiting *crystalline chaos*. A key feature, which is not observed in the absence of modulation [7], is constrained motion: the localized structures preferentially slide back and forth along the phase-locked stripes, *i.e.* following the continuous translational symmetry that is not broken by the modulation.

The phase-locked pattern described above has more stripes per unit length than typical convection patterns. In the absence of modulation this wavelength compression triggers what is known as the skewed-varicose instability, in which one or more stripes are pinched off, forming pairs of dislocations which then separate, thereby removing stripes from the pattern until the local wavenumber is brought back inside the band of preferred periodicities [6]. In our system, where the number and placement of stripes is fixed by the modulation, this mechanism is blocked. Instead, dislocations form cooperative groups confining their far field distortions to small domains with no net topological charge. An orientational distortion of only a single stripe across one wavelength of the modulation (Fig. 2a) provides the smallest possible example of one of these domains. We can understand these localized orientational defects as follows. Dislocations in any stripe pattern generally tend to be pinned by the stripes [3] and, in our system, phase-locking enhances this effect. When dislocations are pinned in adjacent rows, as in Fig. 2a (or its mirror image), a single *kink* (or *antikink*) is formed. The dislocations forming a kink or

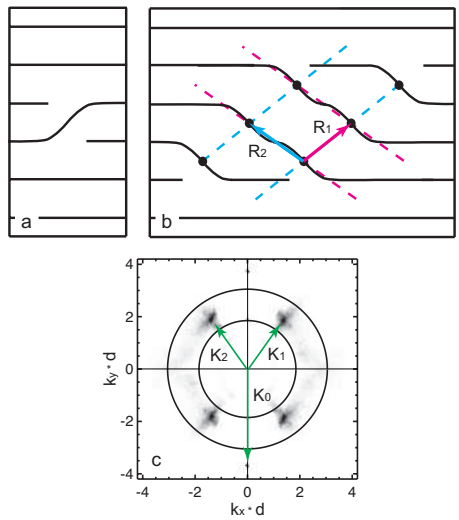

FIG. 2: (a) Kink defect in a phase-locked pattern. (b) Bravais lattice vectors connecting nearest neighbors in a crystalline aggregate; as the kink defects are locked to the modulation, the y-component of each vector equals the modulation wavelength λ. (c) Contrast-enhanced histogram of the corresponding reciprocal lattice basis vectors, showing the relationship of the dominant peaks $\mathbf{K}_1$ and $\mathbf{K}_2$ and the modulation wave vector $\mathbf{K}_0 = (0, -2\pi/\lambda)$ to the stability annulus.

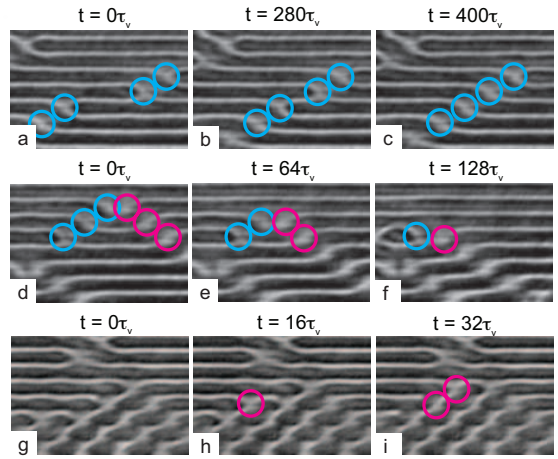

FIG. 3: Time series of shadowgraph images showing (a-c) an aggregation event, in which two chains of antikinks (circled in cyan) approach and lock together to form a longer chain, (d-f) an annihilation event, in which chains of kinks (circled in magenta) and antikinks (circled in cyan) vanish from the pattern through pairwise cancellations, and (g-i) a self-replication event, in which new kinks (circled in magenta) are added at adjacent lattice sites in a crystalline domain. Movie versions of these time series are available at Ref. [21].

antikink cannot separate without creating a gap in the pattern or dislodging a stripe from its locked position. By inhibiting motion, phase-locking provides the system with a new type of coherent structure.

In systems supporting spot-shaped coherent structures, spatially periodic patterns have been interpreted as *crystalline* aggregates of these structures [14, 16, 17]. Here, in the same spirit, we regard the oblique domains of Fig. 1 as mini-crystals constructed from localized orientational defects. The separation vectors connecting adjacent defects provide a local estimate of a real space Bravais lattice basis $\{\mathbf{R}_1, \mathbf{R}_2\}$ for each localized crystalline domain (Fig. 2b). This real space basis has a corresponding reciprocal space basis $\{\mathbf{k}_1, \mathbf{k}_2\}$, defined by the standard relation $\mathbf{k}_i \cdot \mathbf{R}_j = 2\pi\delta_{ij}$ (where $\delta_{ij} = 1$ for $i = j$, and 0 otherwise) [4]. Fixing Ra at $\sim$1.9 Ra_c and averaging results from forty hours of data collection ($57600\tau_v$, where τ_v the vertical diffusion time), we find that these reciprocal basis vectors are statistically concentrated around two locations $\mathbf{K}_{1,2} = (\pm k_x, k_y)$ (and their additive inverses), shown in Fig. 2c together with the modulation wave vector $\mathbf{K}_0$.

The relationships emerging from this analysis are highly illuminating. First, we find that the dominant reciprocal basis vectors, $\mathbf{K}_1$ and $\mathbf{K}_2$, fall well inside the annulus describing the wave vectors of stable stripe patterns in the absence of modulation. Moreover, we find that k_y is equal to one half of the modulation wavenumber $|\mathbf{K}_0|$ and, therefore, the reciprocal basis vectors satisfy a spatial resonance condition, $\mathbf{K}_0 + \mathbf{K}_1 + \mathbf{K}_2 = 0$. This condition can, in fact, be derived a priori from the kink/antikink picture: for any left-right symmetric basis $\mathbf{R}_{1,2} = (\pm a, \lambda)$, locked to the modulation as in Fig. 2b, the standard relation $\mathbf{K}_i \cdot \mathbf{R}_j = 2\pi\delta_{ij}$ leads to $\mathbf{K}_{1,2} = 2\pi(\pm\lambda, a)/(2\lambda a)$ and, given this, $\mathbf{K}_1 + \mathbf{K}_2$ automatically equals $-\mathbf{K}_0 = (0, 2\pi/\lambda)$. Note that the parameter a and its conjugate in reciprocal space, $k_x = \pi/a$ (obtained from the calculation above), are not fixed by the modulation. This free parameter manifests the system's remaining space translational symmetry, parallel to the modulation stripes. By exploiting this freedom, the pattern can use the resonance condition to select crystalline structures with preferred periodicities. Though this condition favors neither $\mathbf{K}_1$ nor $\mathbf{K}_2$, each striped crystal chooses a dominant orientation. This broken reflection symmetry finds a natural explanation in our approach, since the building blocks of each crystal must choose one of two orientations related by a reflection (Fig. 2a and its mirror image). Likewise, since each of these building blocks is associated with a single background stripe, translational confinement of the dynamics becomes a direct consequence of phase-locking and broken translational symmetry.

We emphasize that, while crystallization of coherent structures is observed in a variety of pattern-forming systems, our system has the provocative feature that its localized structures emerge from the (restricted) dynamics of topological defects. An *aggregation* event in which two crystalline chains of antikinks lock together to form a longer chain, observed experimentally, is shown sequentially in Figs. 3a-c. When these chains first come into

contact one pair of dislocations is rapidly annihilated, leaving the net charge unchanged. The reverse process, which fractures larger crystals to form smaller ones by creating and separating a new pair of dislocations, is commonly observed as well. The creation or annihilation of a dislocation pair typically requires only a few τ_v. Thus, the time scales shown in Fig. 3 reflect the robustness that kinks, antikinks, and their aggregates inherit from the modulation. Localized orientational defects of opposite type can also annihilate, returning stripes to their phase-locked positions. Figs. 3d-f show an *annihilation* event in which a "v"-shaped domain contracts through pairwise cancellation of kinks and antikinks. This process, like aggregation, conserves charge and is reversible. The reverse process is quite rare, however, and only occurs in the immediate vicinity of existing kinks and antikinks. This observation suggests that there is an energy barrier associated with the formation of these structures and that proximity to existing structures lowers this barrier.

Though topological charge is conserved, the relative sizes of the kink and antikink subpopulations fluctuate. The process responsible for this fluctuating asymmetry is a jump of a dislocation from one pinning site to a neighboring site; these glide motions are inhibited, as mentioned earlier, but they do occur and are important for the dynamics. When the two dislocations forming a localized orientational defect jump apart, inserting an extra row of the modulation between them, the result of this jump is the formation of an extra localized orientational defect of the same type. This *self-replication* process allows crystals to expand transversely in discrete steps, as shown in Figs. 3g-i, and is what allows the lateral boundaries of the pattern to absorb and emit these structures. Self-replication, like aggregation and annihilation, conserves charge and is reversible. This behavior is distinct from other examples of self-replication, such as cell-division and self-completion [12–14], in that it has a topological origin.

In this Letter, we have presented a completely new localization mechanism native to spatially modulated pattern-forming systems. This mechanism illustrates how, even when individual dislocations are heavily constrained, groups of dislocations may still be free to self-organize and, indeed, acquire a broader palette of generic behaviors to choose from. In this way, applied constraints can both control the emergence of spatiotemporal chaos and make new pattern selection mechanisms possible. In principle, kinks, antikinks, and their aggregates may arise in any spatially modulated stripe-forming system, particularly those which are modeled by Swift-Hohenberg equations [3, 9]. Generalizations of these structures may thus arise in layer-forming systems, such as surfactant lamellae, smectics, and block copolymers, or ecological applications [22]. We hope that our emphasis on the basic concepts of phase-locking, symmetry-breaking, and spatial resonance, rather than system-specific details, will prove useful to other researchers exploring the consequences of spatial forcing and will motivate theoretical studies of this localization phenomenon.

This work was supported by the Max Planck Society and the NSF (DMR-0305151), as well as Cornell's NanoScale Facility (ECS-0335765) and Nanobiotechnology Center (ECS-9876771). We gratefully acknowledge V. Elser, J. Sethna, N. Ouellette, S. Carpenter, N. Ellis, R. Wiener, G. Shaughnessy, and C. Hagedorn for useful discussions and assistance with the apparatus.

* Email: jhm28@cornell.edu
† Email: eberhard.bodenschatz@ds.mpg.de

[1] P. Ball, *The Self-Made Tapestry: Pattern Formation in Nature* (Oxford Univ. Press, New York, 1999).
[2] T. A. Witten, Rev. Mod. Phys. **71**, S367 (1999).
[3] M. C. Cross and P. C. Hohenberg, Rev. Mod. Phys. **65**, 851 (1993).
[4] P. M. Chaikin and T. C. Lubensky, *Principles of condensed matter physics* (Cambridge Univ. Press, New York, 1995).
[5] I. S. Aranson and L. Kramer, Rev. Mod. Phys. **74**, 99 (2002).
[6] E. Bodenschatz, W. Pesch, and G. Ahlers, Annu. Rev. Fluid Mech. **32**, 709 (2000).
[7] S. W. Morris *et al.*, Phys. Rev. Lett. **71**, 2026 (1993); D. Egolf *et al.*, Nature (London) **404**, 733 (2000).
[8] P. Coullet, L. Gil, J. Lega, Phys. Rev. Lett. **62**, 1619 (1989); K. E. Daniels and E. Bodenschatz, Phys. Rev. Lett. **88**, 034501 (2002).
[9] H. Sakaguchi and H. R. Brand, Europhys. Lett. **38**, 341 (1997); C. Crawford and H. Riecke, Physica D **129**, 83, (1999); J. Burke and E. Knobloch, Phys. Rev. E **73**, 056211 (2006).
[10] M. Dennin, G. Ahlers, and D. S. Cannell, Science **272**, 388 (1996).
[11] S. Madruga, H. Riecke, and W. Pesch, Phys. Rev. Lett. **96**, 074501 (2006).
[12] J. E. Pearson, Science **261**, 189 (1993).
[13] K.-J. Lee *et al.*, Nature (London) **369**, 215 (1994).
[14] Y. A. Astrov and Y. A. Logvin, Phys. Rev. Lett. **79**, 2983 (1997).
[15] B. Schäpers *et al.*, Phys. Rev. Lett. **85**, 748 (2000).
[16] P. B. Umbanhowar, F. Melo, and H. L. Swinney, Nature (London) **382**, 793 (1996).
[17] O. Lioubashevski, H. Arbell, and J. Fineberg, Phys. Rev. Lett. **76**, 3959 (1996); O. Lioubashevski *et al.*, Phys. Rev. Lett. **83**, 3190 (1999); R. Richter and I. V. Barashenkov, Phys. Rev. Lett. **94**, 184503 (2005).
[18] J. R. de Bruyn *et al.*, Rev. Sci. Instrum. **67**, 2043 (1996).
[19] J. H. McCoy, Ph. D. thesis, Cornell University, 2007.
[20] S. P. Trainoff and D. S. Cannell, Phys. of Fluids **14**, 1340 (2002).
[21] See EPAPS Document No. [number will be inserted by publisher] for movies showing the dynamics associated with Figs. 1 and 3. For more information on EPAPS, see http://www.aip.org/pubservs/epaps.html.
[22] R. Manor, A. Hagberg, and E. Meron, Europhys. Lett. **83**, 10005 (2008).